HHS Public Access

Author manuscript

Mol Cancer Res. Author manuscript; available in PMC 2020 April 01.

Published in final edited form as:

Mol Cancer Res. 2019 October ; 17(10): 2051–2062. doi:10.1158/1541-7786.MCR-19-0310.

BORIS expression in ovarian cancer precursor cells alters the CTCF cistrome and enhances invasiveness through GALNT14

Joanna C. Hillman[1,Ψ], **Elena M. Pugacheva**[2,Ψ], **Carter J. Barger**[3], **Sirinapa Sribenja**[1], **Spencer Rosario**[4], **Mustafa Albahrani**[3], **Alexander M. Truskinovsky**[5], **Aimee Stablewski**[1], **Song Liu**[6], **Dmitri I. Loukinov**[2], **Gabriel E. Zentner**[7,8], **Victor V. Lobanenkov**[2], **Adam R. Karpf**[3], **Michael J. Higgins**[1]

[1]Department of Molecular and Cellular Biology, Roswell Park Comprehensive Cancer Center, Buffalo NY 14263

[2]Molecular Pathology Section, Laboratory of Immunogenetics, National Institute of Allergy and Infectious Diseases, National Institutes of Health, Rockville, MD 20852

[3]Eppley Institute and Fred & Pamela Buffett Cancer Center, University of Nebraska Medical Center, Omaha, NE, 68198

[4]Department of Cancer Genetics, Roswell Park Comprehensive Cancer Center, Buffalo NY 14263

[5]Pathology, Roswell Park Comprehensive Cancer Center, Buffalo NY 14263

[6]Department of Biostatistics and Bioinformatics, Roswell Park Comprehensive Cancer Center, Buffalo NY 14263

[7]Department of Biology, Indiana University, Bloomington, IN 47405

[8]Indiana University Melvin and Bren Simon Cancer Center, Indianapolis, IN 46202

Abstract

High-grade serous carcinoma (HGSC) is the most aggressive and predominant form of epithelial ovarian cancer and the leading cause of gynecological cancer death. We have previously shown that *CTCFL* (also known as *BORIS*, Brother of the Regulator of Imprinted Sites) is expressed in most ovarian cancers, and is associated with global and promoter-specific DNA hypomethylation, advanced tumor stage, and poor prognosis. To explore its role in HGSC, we expressed *BORIS* in human fallopian tube secretory epithelial cells (FTSEC), the presumptive cells of origin for HGSC. *BORIS*-expressing cells exhibited increased motility and invasion, and *BORIS* expression was associated with alterations in several cancer-associated gene expression networks, including fatty acid metabolism, TNF signaling, cell migration, and ECM-receptor interactions. Importantly, *GALNT14*, a glycosyltransferase gene implicated in cancer cell migration and invasion, was highly induced by BORIS, and *GALNT14* knockdown significantly abrogated BORIS-induced cell motility and invasion. In addition, *in silico* analyses provided evidence for *BORIS* and

Correspondence: Adam R. Karpf, University of Nebraska Medical Center, 42nd and Emile Streets, Omaha, NE, 68198, 402-559-6115, FAX 402-559-4651, adam.karpf@unmc.edu; Michael J. Higgins, Roswell Park Comprehensive Cancer Center, Elm and Carlton Streets, Buffalo, NY 14263, 716-845-3582 FAX 716-845-5908, michael.higgins@roswellpark.org.

Ψ These authors contributed equally to this work.

Conflicts of Interest: The authors declare no conflict of interest.

GALNT14 co-expression in several cancers. Finally, ChIP-seq demonstrated that expression of *BORIS* was associated with *de novo* and enhanced binding of CTCF at hundreds of loci, many of which correlated with activation of transcription at target genes, including *GALNT14*. Taken together, our data indicate that *BORIS* may promote cell motility and invasion in HGSC via upregulation of *GALNT14*, and suggests *BORIS* as a potential therapeutic target in this malignancy.

Keywords

CTCFL; *BORIS*; *CTCF*; *GALNT14*; ovarian cancer; cancer testis gene; chromatin remodeling; cell motility; invasion

Introduction

Although ovarian cancer accounts for less than 2% of all new cancer cases in American women, it is the leading cause of gynecological cancer death, claiming the lives of more than half of all women diagnosed within 5 years. The discordance between prevalence and prognosis is primarily due to its advanced stage at diagnosis, as over 80% of patients present with disseminated cancer that is often resistant or refractory to standard treatment measures. HGSC is the most aggressive and most predominant form of epithelial ovarian cancer (EOC), making up more than 70% of diagnosed cases. Molecular analysis of a large number of HGSC in TCGA uncovered a high frequency of DNA copy number alterations (CNA) and almost ubiquitous occurrence of *TP53* mutations, as well as a low but statistically significant frequency of alterations in *BRCA1*, *BRCA2*, *NF1*, *RB1*, and *CDK12* [1]. Pathway analysis implicated defective homologous recombination in approximately half of HGSC and the activation of both NOTCH and FOXM1 signaling [1, 2].

Although the ovarian surface epithelium (OSE) was originally thought to contain the cell of origin, it is now recognized that most HGSCs originate in secretory cells of the distal fallopian tube (fimbriae) and only later metastasize to the ovary. Providing evidence for this paradigm shift, a large proportion of patients with HGSC have noninvasive lesions called serous tubal intraepithelial carcinoma (STIC) in their fallopian tubes that are histologically similar to and carry identical mutations (including TP53) and expression profiles as HGSC [3]. STIC has been found in patients who underwent prophylactic salpingo-oophorectomy in the absence of any invasive carcinoma but were known carriers of BRAC1/2 predisposition mutations [4], indicating that this lesion can predate invasive cancer. Moreover, our previous DNA methylome analyses demonstrated that the methylation profile of HGSCs and fallopian tube epithelia (FTE) are more similar than are HGSCs and OSE [5]. These findings prompted the development of immortalized fallopian tube secretory epithelial cells (FTSEC) derived from the fimbrial region as a more physiologically relevant experimental model of the disease [6]. The validity of this model was supported by the demonstration that ectopic expression of cyclin E1 (*CCNE1*), which is associated with poor survival in HGSC, imparted malignant properties to untransformed fallopian tube epithelial cells when TP53 function was abrogated, leading to an accumulation of DNA damage and altered transcription of DNA damage response genes related to DNA replication stress [7].

We have previously shown that *BORIS* (*CTCFL*) is expressed in a large proportion of EOC and its expression is associated with global genomic DNA hypomethylation and *BORIS* promoter DNA hypomethylation [8]. Importantly, a significant association was found between *BORIS* expression, increased tumor stage, and poor prognosis [9]. *BORIS* is a cancer germline (CG) or cancer testis (CT) antigen gene, primarily expressed in the germline under normal circumstances and abnormally activated in many malignancies [10]. Indeed, BORIS is one of the most commonly activated CG genes in cancer [11] and has been proposed as an activator of other CG genes [12], making it an attractive immunotherapy target [13].

BORIS is the sole paralog of CTCF (CCCTC-binding factor), a multifunctional DNA binding protein [14]. BORIS and CTCF share high homology in their central zinc finger core and can potentially bind identical or similar DNA sequences; however, ChIP-seq experiments in cancer and germ cells have shown that BORIS binds only a subset of CTCF binding sites [15] actually consisting of two closely located CTCF binding motifs (termed 2xCTSes) either as a CTCF-BORIS heterodimer or a BORIS homodimer [15]. The 2xCTSes are generally enriched in active chromatin marks including H3Kme2, H3Kme3, H3K27ac, H3K79me2 and H3K9ac, in addition to the histone variant H2A.Z [15, 16]. Unlike single-motif CTCF target sites (1xCTSes), which are suggested to have insulator function, 2xCTSes are preferentially found at regions of open chromatin such as active promoters and enhancers, in both cancer and germ cells [15]. Interestingly, 2xCTSes are also enriched in genomic regions that escape the replacement of histones by protamines in human and mouse sperm [15].

Despite the high degree of similarity in their DNA binding domains, the N- and C-terminal domains of CTCF and BORIS are highly divergent suggesting that, once bound, these two proteins may elicit distinct effects [14]. CTCF is highly conserved, ubiquitously expressed, and essential for normal development, as evidenced by embryonic lethality of whole body CTCF knockout in mice [17]. Documented roles for CTCF include widespread transcriptional regulation, genomic imprinting, chromatin domain insulation, and X-chromosome inactivation (reviewed in [18]). The multifunctionality of CTCF often hinges on its utility as an architectural protein, maintaining genomic stability and facilitating gene regulatory interactions through chromosome loop formation in conjunction with the cohesin complex [19]. In contrast to *CTCF*, the function(s) of *BORIS* in the male germline and in cancer cells is less established. The exclusive expression of *BORIS* in the male germline, and defective spermatogenesis in *BORIS* knockout mice, suggest that the normal function of BORIS is to regulate male germ cell development. This function may be due to its regulating expression of the important testis-specific genes *Gal3st* and *Prss50* [15, 20, 21] possibly by cooperating with CTCF (at 2xCTSes) and other testis-specific transcription factors [22]. In cancer, BORIS has been proposed to be an oncogene with various studies demonstrating its activity in repressing tumor suppressor genes including CTCF and inducing other oncogenes [23]. BORIS has been shown to induce pro-tumorigenic phenotypes in cell line models [24–26], including increased cellular proliferation [27–29] and invasion [26, 29]. Although the mechanism(s) of action of BORIS is still being elucidated, it may function in a dominant-negative fashion by displacement of CTCF and the reorganization of the chromatin landscape [15, 30] thus impacting gene expression and contributing to the cancer phenotype.

Consistent with this idea, our previous studies showed that an elevated BORIS/CTCF expression ratio correlated with disease progression in ovarian cancer [9].

In the current study we assessed the phenotypic and molecular changes that BORIS expression imposes on a physiologically relevant model of HGSC precursor cells. BORIS was expressed in FT282 cells, an immortalized non-transformed cell line derived from FTSEC, the proposed initiating cells of many HGSCs [7]. Ectopic expression of *BORIS* in FT282 cells induced changes indicative of cellular transformation including increased migration and invasion through Matrigel. Phenotypic changes were accompanied by significant alterations in gene expression and alteration of key cancer associated pathways. In particular, BORIS induced expression of the cancer-associated glycosyltransferase *GALNT14* gene, which contributed to the downstream invasive phenotype. Moreover, BORIS was directly implicated in many of the observed gene expression changes, as its binding was enriched at differentially expressed genes (DEGs). Finally, ectopic expression of BORIS in FT282 cells was associated with both quantitative and qualitative increases in genomic CTCF binding. Taken together, our results support a role for *BORIS* in increasing the invasive potential of HGSC precursor cells. These data, coupled with widespread increased expression of *BORIS* in HGSC, suggests that BORIS is a potential therapeutic target in this malignancy.

Materials and Methods

FTE cell culture and ectopic BORIS expressing cell line

A clonal derivative of FT282 was generated a previously described [31], and cultured in DMEM/Ham's F-12 50/50 Mix (DMEM:F12) without L- glutamine (Corning) with 10% FBS (Peak Serum) and 1% Penicillin-Streptomycin (Gibco). To generate a BORIS expressing FT282 cell line, a CpG-free BORIS cDNA [15] was cloned into SparQ IRES lentivector containing green fluorescent protein (GFP) (System Biosciences). FT282 cells were transduced with BORIS containing lentivirus or empty vector (EV) in the presence of 8μg/mL polybrene. Infected cells were propagated for 14 days and sorted to obtain GFP positive cells containing lentivirus.

Protein extraction and western blotting

Cells at approximately 80% confluency in 6 well plates were washed 2x with 1ml ice-cold PBS containing protease inhibitors (Pierce™ Protease Inhibitor Mini Tablets, EDTA Free) and lysed in 150μl, high-salt RIPA buffer (50mM Tris-HCl pH 7.4, 0.5M NaCl, 0.25% Deoxycholic acid, 1% NP-40, 1mM EDTA, 0.1% SDS) containing protease inhibitors. Lysates were sonicated on ice for two 15 second intervals with cooling between cycles. Samples were vortexed and quantified using the Pierce BCA Protein Assay Kit (Thermo Fisher Scientific). Twenty (20) μg of protein was prepared with 1% β-mercaptoethanol and 1x lithium dodecyl sulfate (LDS) sample buffer (NuPAGE), separated by SDS-PAGE and transferred to PVDF membranes (Bio-Rad). Membranes were blocked with 5% nonfat dry milk (NFDM) in 0.1M PBS containing 0.1% Tween-20 (PBST) and incubated with primary antibody overnight in 5% NFDM at 4°C. Membranes were washed 3x in PBST (8 minutes each at RT). Membranes were then incubated with secondary antibody diluted in 5% NFDM

for 1 hour at RT, followed by three washes in PBST. The signal was detected using Pierce™ ECL Western Blotting Substrate (Thermo Fisher Scientific) and images captured on the Bio-Rad ChemiDoc Touch Imaging System. Primary antibodies were anti-human BORIS mouse monoclonal antibody (1:1000) [15], GALNT14 rabbit polyclonal antibody (1:1000) (Proteintech: 16939-1-AP) and ACTB mouse monoclonal (1: 10,000) (Sigma). Anti-mouse (#55550) and anti-rabbit (#55676) secondary antibodies were from MP Biomedical. Secondary antibodies were used at a 1:2000 dilution.

Proliferation assays

Cells were grown in 100 μl of complete medium in 96 well plates. Eight (8) technical replicates for each cell line/treatment were seeded onto 5 separate plates, one for each time point. Every 24 hours one plate was processed. The Sulforhodamine B (SRB) assay was carried out as described [32].

Transwell migration and invasion assays

FT282-BORIS and FT282-EV cells were grown to 60% confluency in complete medium; 24 hr prior to trypsinization the medium was replaced with serum-free medium (DMEM:F12 + 1% Penicillin-Streptomycin). Fifty thousand ($5X10^4$) cells in 500μl serum-free media were pipetted into the top of transwell inserts (8 micron pores, BD Biosciences) in a 24 well plate. Five hundred (500) μl of complete medium (chemoattractant) was pipetted into the bottom chamber. After 18 hours, cells were removed from the top surface of the membrane with a cotton swab and inserts fixed in 100% methanol, washed and stained in 0.2% crystal violet. Dried membranes were mounted onto glass slides for microscopic evaluation. Experiments were performed in triplicate transwells and quantified by averaging the number of cells per 20x field of view counting 4 fields per chamber. Invasion assays were carried out in a similar manner except inserts coated with Matrigel were used and assays were carried out for 22 hours.

Propidium Iodide staining/cell cycle analysis

Approximately $2X10^6$ cells were washed twice in cold PBS and resuspended in 300 μl of PBS. Cells were fixed by adding 700 μl of 100% ethanol (EtOH) dropwise while vortexing. Fixed cells were stored at −20°C until staining was performed. Cells were washed in PBS and stained with 50 μg/ml propidium iodide at 4°C for 1 hour, passed through a 0.2 micron filter and analyzed on an LSR Fortessa A. instrument. Cell cycle analysis was done using ModFit 4.1.

RNA-sequencing, DEG identification, and pathway analysis

Sequencing libraries were prepared from 1μg total RNA using the TruSeq Stranded Total RNA kit (Illumina). Library preparation, sequence enrichment and sequencing were carried out by the RPCCC Genomics Shared Resource using an Illumina HiSeq2500. FASTQ files were mapped to the UCSC Human reference (build hg19) using TopHat2 with the default parameter setting of 20 alignments per read and up to two mismatches per alignment. The aligned reads (BAM files) were then analyzed with Cufflinks 2.0.0 to estimate transcript relative abundance using the UCSC reference annotated transcripts (build hg19). The

expression of each transcript was quantified as the number of reads mapping to a transcript divided by the transcript length in kilobases and the total number of mapped reads in millions (FPKM). GO analysis was performed in R 3.5.1 with clusterProfiler 3.8.1. Biological process annotation was performed with the enrichGO() command and redundant annotations were collapsed with simplify(up_ego, cutoff=0.7, by="p.adjust", select_fun=min) prior to plotting. Full GO results are provided in Supplementary Table 2. Significantly dysregulated genes ($p<0.006$, $logFC> |0.25|$), were then tested for pathway enrichment utilizing DAVID (https://david.ncifcrf.gov) and the KEGG database (http://www.genome.jp/kegg/) and the Reactome (https://reactome.org/) database. Complete RNA-seq data is available in GEO under accession number GSE131931.

Reverse transcriptase quantitative polymerase chain reaction (RT-qPCR)

One microgram (1μg) of DNase-treated RNA was converted to cDNA using the iSCRIPT Advanced cDNA Synthesis Kit (Bio-Rad). cDNA was diluted 1:10 with water for use in subsequent RT-qPCR reactions. RT-qPCR was performed using the CFX96™ Real-Time PCR Detection System (Bio-Rad) with SsoAdvanced™ Universal SYBR® Green Supermix (Bio-Rad). Primers used for qPCR were designed using Beacon Designer (Premier Biosoft) and sequences included in Supplmentary Table 7. *HPRT1* mRNA levels were assayed as an endogenous control.

siRNA knockdown of GALNT14

Knockdown of *GALNT14* was by transient transfection of *Silencer*® Select siRNA targeted against *GALNT14* (ThermoFischer Scientific, assay s35936); the *Silencer*® Select Negative Control No. 1 was used as a baseline control. Cells were grown to approximately 80% confluency in 6 well dishes. For each transfection 3μl of Lipofectamine RNAiMAX reagent was added to 150μL of Opti-MEM medium followed by 30 pmol of siRNA. The diluted siRNA (150μL) was added to the diluted Lipofectamine RNAiMAX reagent and incubated for 5 minutes in a heat block at 23°C. Two hundred-fifty (250μL) of the siRNA Lipofectamine RNAiMAX complex was then added dropwise to the cells. Cells were harvested for protein 48 hours after transfection and *GALNT14* knock down was confirmed by western blot.

ChIP-sequencing

ChIP-seq and bioinformatics analysis was performed essentially as described using approximately 10^8 cells [15]. Formaldehyde-fixed chromatin was sheared to 200– 500 bp (Bioruptor), incubated overnight with DiaMag magnetic beads (Diagenode, Inc.) and CTCF or BORIS monoclonal or polyclonal antibodies [15] and DNA isolated from precipitated chromatin. ChIP DNA was amplified using a TruSeq ChIP Sample Preparation Kit (Illumina, Inc., USA) and used for single end sequencing on an Illumina Genome Analyzer. Sequences were aligned with Bowtie and peaks called using MACS; the Peak Splitter was used to call sub-peaks and summits of peaks and improve peak resolution. ChIP-seq data were visualized using IGV. Peak overlaps between CTCF and BORIS ChIP-seq data sets were determined with BedTools Suite. Peaks were defined as overlapping if at least 1 bp of reciprocal peaks intersect (CTCF&BORIS); the remaining peaks were defined as non-overlapping (CTCF-only and BORIS-only). Normalized tag density profiles were generated

using the BedTools coverage option from the BedTools Suite, normalized to the number of mapped reads, and plotted in Microsoft Excel. The heatmaps were generated using the seqMINER 1.3.3. We used either k-means ranked or linear method for clustering normalization. The summits of either CTCF or BORIS peaks were extended ±5 kb. seqMINER was also used to generate the average profiles of read density for different clusters. Position weight matrices for CTCF and BORIS bound regions were searched using Multiple EM for Motif Elicitation (MEME). The sequences under the summit of either CTCF or BORIS peaks extended 100 bp upstream and downstream were used for motif discovery. We ran MEME with parameters (− mod oops-revcomp -w 20) to identify 20-bp-long motifs considering both DNA strands. To analyze the occurrence of CTCF motifs in the sequences occupied by CTCF or BORIS, or both proteins, FIMO software (MEME suite) was employed with default parameters. The position weight matrices found for CTCF binding regions by MEME were used for FIMO software. Each CTCF motif occurrence had a p value < 0.0001 in the sequences of 200 bp around the summit of either CTCF (CTCF-only, CTCF&BORIS bound regions) or BORIS (BORIS-only bound regions) peaks. Genomic distribution of CTCF and BORIS ChIP-seq peaks relative to reference genes was performed using the Cis-regulatory Element Annotation System (CEAS). Complete ChIP-seq data is available in GEO under accession number GSE131931.

Results

BORIS expression in epithelial ovarian cancer (EOC) correlates with increased stage and decreased survival

We previously showed that *BORIS* expression in EOC correlated with advanced tumor stage and decreased survival; interestingly, this correlation was even more significant when the ratio of *BORIS*/*CTCF* mRNA expression was used in the analysis. Furthermore, a significant correlation was observed between BORIS promoter hypomethylation, increased tumor stage and poor prognosis [9]. To corroborate these findings in an independent and larger dataset, we queried CSIOVDB (Ovarian Cancer Database of Cancer Science Institute Singapore), a microarray-based gene expression database of EOC [33]. Analyses showed that *BORIS* expression is significantly higher in fallopian tube carcinoma (“FTE tumors”) and ovarian carcinomas (“Tumors”) compared to normal fallopian tube epithelium (FTE) and ovarian surface epithelium (OSE) (Supplementary Fig. 1). Moreover, *BORIS* expression is highest in serous tumors compared to other EOC subtypes (Supplementary Fig. 2A). Consistent with our previous findings, *BORIS* expression was significantly higher in advanced stage (Fig. 1A) and higher-grade tumors (Supplementary Fig. 2B). A similar analysis of 47 ovarian cancer cell lines in the Cancer Cell Line Encyclopedia (CCLE) showed no significant differences in levels of BORIS expression across histological subtypes from which the cell lines were derived (Supplementary Fig. 2C); stage and grade information was not available. Also consistent with our earlier study, *BORIS* expression correlated with reduced disease-free and overall survival (Fig. 1B). When the ratio of *BORIS*:*CTCF* expression was used in these analyses, the same associations were observed (Supplementary Fig. 3). We also analyzed RNA-seq data from The Cancer Genome Atlas (TCGA) and found that ovarian cancers (i.e. HGSC) exhibited the highest expression of *BORIS* compared to other cancers (data not shown). However, no correlation was observed

between *BORIS* mRNA expression, or *BORIS*:*CTCF* mRNA expression ratio, and overall survival in HGSC (Supplementary Fig. 4). This was also true when TCGA microarray expression data was used (not shown). The discrepancy between CSIOVDB and TCGA is likely explained by the fact that CSIOVDB data contains all EOC subtypes while TCGA data is composed solely of HGSC. Indeed, when similar analysis was carried out using only the serous carcinoma samples in CSIOVDB, no correlation with survival was observed (Supplemental Fig.5) consistent with increased expression of *BORIS* in HGSC (Supplementary Fig. 2A).

Ectopic expression of BORIS in FTE cells induces cellular changes typical of cellular transformation

To determine the impact of ectopic BORIS expression in a physiologically relevant *in vitro* model of HGSC, we employed a clonal derivative of the immortalized, non-transformed human fallopian tube epithelial cell line, FT282 originally described by Karst et al. [7]. The FT282 cell line was established from normal human FTE cells immortalized with the catalytic subunit of human telomerase, telomerase reverse transcriptase (TERT) and carrying mutant *TP53R175H,* a dominant negative mutation, as TP53 mutations are ubiquitous in early stages (i.e. STICs) of HGSC transformation [34]. A clonal derivative of FT282 cells (FT282-c11)[31] was infected with the SparQ IRES lentivector-GFP containing a BORIS cDNA or the empty vector (EV) and cells sorted for GFP to enrich for infected cells. Western blot analyses confirmed high BORIS protein expression in FT282-BORIS, but not FT282-EV cells (Fig. 2A).

To address whether BORIS expression induced phenotypic changes associated with transformation, FT282-BORIS and FT282-EV cells were assayed for changes in cellular morphology, proliferation, migration and invasion. Microscopic evaluation failed to reveal differences in morphology between FT282-BORIS and FT282-EV cells (Supplementary Fig. 6A) and their appearance was similar to that of early passage immortalized FTSECs [6]. BORIS expression did not alter cellular proliferation, as assayed by the SRB assay (Supplementary Fig. 6B) or the MTS assay (not shown). However, cell cycle analysis (Fig. 2B) demonstrated that FT282-BORIS cells had a significantly smaller proportion of cells in G1 compared to FT282-EV cells ($p = 0.02$), a slightly larger (but not statistically significant) proportion of cells in S-phase ($p = 0.32$), and more than twice the proportion of cells in G2/M ($p = 0.0014$), suggesting cell cycle arrest at the G2/M checkpoint (Fig. 2C). Notably, cell migration was significantly enhanced in the FT282-BORIS cells as assayed by transwell migration assays (Fig. 2D); furthermore, FT282-BORIS exhibited twice the level of invasion through Matrigel compared to the FT282-EV control (Fig. 2E). Taken together, these results indicate that BORIS expression changed the behavior of FT282 cells, driving them towards a transformed phenotype.

Ectopic BORIS expression modulates expression of cancer-associated genes and pathways

During spermatogenesis BORIS acts as a transcriptional regulator of several essential testis-specific genes, Gal3st and Prss50 [15, 20]. To access the impact of ectopic BORIS expression in FTE cells, we performed RNA-sequencing (RNA-seq) analysis in FT282-

BORIS cells compared to the FT282-EV control which revealed substantial differences in gene expression between the cell populations (Fig. 3A). The total number of differentially expressed genes (DEGs) in FT282-BORIS compared to FT282-EV was 1656, including 773 genes significantly upregulated and 883 genes significantly downregulated ($p < 0.006$) (Supplementary Table 1). To gain insight into the functional significance of these changes, we performed gene ontology (GO) analysis. Consistent with the increase in migration observed in FT282-BORIS cells, upregulated genes were significantly enriched for biological processes including “regulation of chemotaxis” and “positive regulation of cell migration” while downregulated genes were enriched for processes such as “extracellular matrix organization” and “cell-substrate interaction” (Fig. 3B, Supplementary Table 2).These observations suggest that BORIS enhances FT282 cell motility by upregulating positive regulators of cell motility and downregulating genes involved in cell adhesion.

It might be anticipated that the more differentially expressed genes in a biological process may be driving identification of the GO category. Using this criterion, a number of genes from several different GO categories (Supplemental Table 2) were chosen to validate the RNA-seq data using RT-qPCR. These included 6 genes upregulated in BORIS-expressing cells, *GALNT14* and *CHSY3* (glycoprotein biosynthesis), *SERPINB2* and *PCOLCE2* (regulation of peptidase activity), *ITGA4* (positive regulation of cell migration), and *CXCL2* (regulation of cell migration and chemotaxis), as well as 4 genes downregulated in FT282-BORIS cells, *KLK5* (ECM organization), *SFRP1* and *IGFBP5* (gland development), and *BCAM* (cell substrate adhesion). All 6 upregulated genes were validated by RT-qPCR (Fig. 3C), while 3 of 4 of the downregulated genes also exhibited decreased expression by RT-qPCR (Fig. 3D); *IFGBP5* did not validate possibly because of cross reaction with other *IGFBP* gene family members.

KEGG pathway analysis revealed several cancer-associated pathways significantly impacted by ectopic BORIS expression (Supplementary Table 3). In this analysis, the pathway for biosynthesis of unsaturated fatty acids was the most enriched for DEGs upregulated in FT282-BORIS cells; fatty acids are essential for cancer cell proliferation due to a high demand for lipids [35]. Consistent with this, several downregulated genes are involved in fatty acid degradation. In addition, the tumor necrosis factor (TNF) signaling pathway was amongst the most highly upregulated. The NF-kappa-B (NFKB) signaling pathway, which is activated by proinflammatory cytokines, including those in the TNF pathway was also significantly upregulated as well as the cytokine-cytokine receptor interaction and the rheumatoid arthritis pathway. Among pathways enriched for genes downregulated in FT282-BORIS cells were genes involved in signaling of the p53 tumor suppressor gene. Notably, a separate pathway analysis using the Reactome database also identified several inflammatory pathways including interleukin-10 signaling, chemokine receptors, and the inflammasome pathway as enriched in upregulated genes in FT282-BORIS cells, as well as several pathways related to p53 signaling enriched for downregulated genes (Supplementary Table 4). Consistent with the observed increases in migration and invasion, several related pathways were also enriched for DEGs; for example KEGG pathways for adherens junction and focal adhesion were enriched for a large number of genes downregulated in FT282-BORIS cells, some of which (e.g. *WASF3*, *ACTN2*, *TCN*, *VCL*, *ZYX*) are known to enhance cell motility or metastasis when lost in certain cell types (for example [36]). Among

upregulated genes, the “Mucin type O-Glycan biosynthesis” pathway was significantly enriched in the KEGG analysis (Supplementary Table 3). Similarly, analysis of upregulated DEGs in the Reactome database revealed enrichment in pathways for “O-linked glycosylation of mucins” (Supplementary Table 4). Abnormal glycosylation, which is often attributed to deregulated expression of glycosytransferases, is a common feature of human cancers and affects a number of cellular properties including proliferation, apoptosis, differentiation, migration, invasion, transformation, and immune responses [37]. Thus, BORIS expression in normal FTE cells resulted in a deregulation of multiple cell pathways related to cancer development and progression.

BORIS induces expression of GALNT14 in FTE cells which contributes to the migratory and invasive phenotype

GALNT14, a member of the Mucin type O-Glycan biosynthesis pathway, was the most highly induced gene (log2 [fold change] = 5.85) (Supplementary Table 1), a finding confirmed by RT-qPCR (Fig. 3C). Western blot analysis confirmed that GALNT14 protein was also significantly upregulated in FT282-BORIS cells compared to FT282-EV (Fig. 4A). In addition, we found that *BORIS* and *GALNT14* were co-expressed in several cancer datasets, providing further evidence for a link between these two genes (Supplementary Table 5).

Based on the transcriptional induction of *GALNT14*, and its proposed involvement in cancer cell migration and invasion in ovarian cancer [38], we sought to determine if the BORIS-associated increase in cellular migration and invasion was related to the observed increase in expression of *GALNT14*. FT282-BORIS cells were transfected with siRNA targeted against *GALNT14* mRNA, or with a non-targeting negative control. GALNT14 protein was markedly reduced by siRNA knock-down (KD) (Fig. 4B) and this correlated with significantly decreased migration (Fig. 4C), supporting the notion that the GALNT14 glycosyltransferase is involved in the BORIS associated increase in cell motility. Moreover, KD of *GALNT14* significantly diminished the ability of FT282-BORIS cells to invade through Matrigel compared to the negative control (Fig. 4D). These results implicate *GALNT14* as a contributor to BORIS-induced cellular and molecular changes in FT-282 cells. Taken together, these results corroborate previous studies implicating BORIS in upregulation of inflammatory genes and pathways [15] as well as provide a novel link between BORIS expression and aberrant o-linked glycosylation of mucins, which may function in cell migration and invasion.

BORIS binding is enriched at the promoters of deregulated genes

In order to investigate the genomic targets of ectopically expressed BORIS, and to compare BORIS binding with CTCF occupancy, we performed genome-wide ChIP sequencing (ChIP-seq) in FT282-BORIS and FT282-EV cells. ChIP-seq identified a total of more than 47,000 CTCF binding sites (ChIP-seq peaks) in the two cell populations with 95% present in both FT282-BORIS and FT282-EV cells. In addition, almost 24,000 BORIS peaks were identified in FT282-BORIS cells (Fig. 5A, left-hand panel). Overlapping of CTCF and BORIS ChIP-seq peaks in FT282-BORIS cells revealed three classes of differential occupancy: 29,112 sites bound by CTCF alone (CTCF-only), 15,513 sites bound by both

CTCF and BORIS (CTCF/BORIS shared), and 8,140 sites bound by BORIS alone (BORIS-only) (Fig. 5A, right-hand panel). In a previous study using three cancer cell lines that express BORIS endogenously, we showed that BORIS preferentially binds and forms CTCF-BORIS heterodimers at 2xCTSes [15]. Thus, to determine if ectopically-expressed BORIS in FT282-BORIS cells was also associated with 2xCTSes, we carried out CTCF motif analysis using FIMO (MEME suite) within the sequence 100 bp upstream and downstream of the summit of the top 1000 CTCF, CTCF/BORIS shared or BORIS (BORIS-only) peaks (Fig. 5B, left-hand panel). More than one CTCF motif was identified under 53% of BORIS-only peaks and 42% of CTCF/BORIS shared peaks compared to only 12% for CTCF-only peaks (Fig. 5B, right-hand panel), thus confirming previous findings that BORIS preferentially occupies 2xCTSes either together with CTCF or alone. Also in agreement with previous work [15], BORIS binding in the FT282-BORIS cell line was enriched at promoter regions (defined as plus or minus 2kb from the transcription start sites [TSS]), while CTCF-only sites were relatively depleted at promoters and comparatively enriched at intergenic regions (Fig. 5C). Consistent with this, and in contrast to CTCF alone, BORIS preferentially bound to CpG islands (CGI) (Fig. 5D). Compared to genes not affected by BORIS expression, binding of BORIS was significantly enriched at both upregulated and downregulated DEGs, 83% and 61% respectively (Fig. 5E) suggesting direct involvement of BORIS in gene regulation at these loci. Importantly, upregulation of *GALNT14* was accompanied by BORIS binding at sites within the promoter and gene body (Fig. 5F). Similarly, upregulation of *BIRC2*, a component of the TNF signaling pathway, was accompanied with increased binding of BORIS at its promoter (Supplementary Fig. 8). Taken together, these results further demonstrate that, when aberrantly expressed, BORIS binds to a subset of CTCF bound sites (CTCF/BORIS), as well as a number of sites not bound by CTCF (BORIS-only). Moreover, comparison of BORIS binding and RNA-seq data suggests that, in many cases, BORIS is influencing the transcription of DEGs as a consequence of direct promoter occupancy.

CTCF ChIP-seq in the FT282-BORIS and FT282-EV lines also suggested a second mechanism beyond competition at CTCF binding sites by BORIS at genomic loci already bound by CTCF. Compared to FT282-EV cells, more than 500 loci in BORIS expressing cells exhibited enhanced binding of CTCF, defined as a tag density more than three times higher in BORIS expressing cells compared to FT282-EV (Supplementary Fig. 7). In some cases, CTCF binding was clearly evident in FT282-BORIS cells but undetectable in BORIS-EV cells and thus appeared as “new” CTCF-binding sites (Fig. 5F, Supplementary Fig. 8). For example, the *GALNT14* gene showed increased CTCF binding at its promoter and a novel CTCF binding site in the gene body (Fig. 5F), indicating that increased CTCF occupancy may be important for its increased expression in FT282-BORIS cells. Interestingly, only about 50% of these new or enhanced CTCF binding sites were also bound by BORIS in FT282-BORIS cells. These new or enhanced CTSes appeared to be nonrandom with respect to genomic location. More than two-thirds (382/561) of them overlap with known genes, 74 of which are DEGs. Fifty-three (53) of these 74 (~72%) DEGs were upregulated at the mRNA level in FT282-BORIS cells, while 21 (~28%) were downregulated (Supplementary Table 6). This phenomenon indicates that BORIS binding

may lead to a more open chromatin conformation at upregulated DEGs by making these regions more accessible to CTCF binding.

Discussion

Identification of oncogenic drivers of HGSC is expected to lead to new therapeutic targets in this malignancy. Our earlier findings that expression of BORIS was positively correlated with advanced stage disease and poor prognosis of ovarian cancer patients [9] suggested that this CT gene might be an oncogene in this malignancy. Here, we corroborated these findings by showing in an independent dataset (CSIOVDB), that BORIS expression is highly expressed in HGSC and correlates with advanced stage and reduced disease-free and overall survival. The correlation is even more significant when the ratio of BORIS/CTCF mRNA is used in the analysis possibly reflecting the competitive nature of BORIS and CTCF binding.

Expression of BORIS in human FT282 cells, a physiologically relevant cell culture model of HGSC precursor cells in the fallopian tube [6, 7] resulted in enhanced cellular migration and invasion. Changes in cell cycle progression were also observed, as BORIS expression led to cell cycle arrest at G2/M. Since CTCF has previously been shown to regulate cell cycle progression [39, 40] it might be anticipated that this function could be impaired by BORIS-induced disruption of CTCF regulation at key cell cycle genes. Moreover, this phenotype is consistent with previous studies linking BORIS expression to deregulation of the cell cycle [26]. Alternatively, cell cycle arrest in BORIS expressing cells may reflect DNA damage due to disruption of CTCF function in limiting oxidative stress [41]. Related to this, RNA-seq analysis indicated a significant upregulation in ataxia telangiectasia mutated (*ATM*) mRNA in BORIS expressing cells [42]. There was also significant upregulation of genes involved in inflammatory pathways and the O-linked glycosylation of mucins, including a more than 50-fold (RNA-seq) upregulation of *GALNT14*, a glycosyltransferase with an established link to ovarian and breast cancer cell migration [38, 43]. siRNA knockdown of *GALNT14* partially abrogated both cellular migration and invasion in FT282-BORIS cells, supporting its role as a downstream effector of these BORIS-induced phenotypes. Importantly, based on ChIP-seq analysis, *GALNT14* is a direct target of BORIS. Although *BORIS* and *GALNT14* expression appears to be correlated in several other cancer types, this association was not observed in primary HGSC (Supplementary Table 5). One possibility for this inconsistency is that BORIS regulates *GALNT14* expression only early on in HGSC progression; alternatively, *BORIS* and *GALNT14* may be co-expressed in only a subset of tumor cells, similar to the intratumor heterogeneity observed previously for other CT genes [44]. *GALNT14*, and most of the other genes examined by RT-qPCR (Fig. 3C&D), exhibited co-expression (i.e. maintained high log odds ratios in co-occurrence and mutual exclusivity analysis, cBioPortal) in TCGA ovarian cancer expression data. This is consistent with our finding that all but one of these genes (*CXCL2*) bound BORIS and CTCF at their promoter regions and/or at intragenic regions in BORIS-expressing FT282 cells. Despite this, only expression of *CHSY3* and *SERPINB2* (both upregulated) mirrored BORIS expression with respect to increased expression in later stage and higher grade tumors in the CSIOVDB database; similarly, only increased expression of *CHSY3* and *SERPINB2* correlated with either overall or disease-free survival (Supplemental Fig. 9) similar to BORIS expression

(Fig. 1). It may be that other BORIS transcriptional targets, or the overall chromatin state induced by BORIS, are driving the survival association for BORIS.

In some contexts, BORIS has been implicated in the activation of other CT antigen (CTA) genes [12, 45]; however, in our study only 26 of 1019 identified CTA genes [11] were significantly upregulated in FT282-BORIS cells (not shown), a finding consistent with other studies that have failed to verify BORIS-mediated induction of CT genes [46, 47]. BORIS expression had no detectable effect on FT282 cell proliferation. This might be explained by the unique pattern of progression of ovarian cancer, in that initial cellular transformation may begin in the FTE, but the ovary is often the site of the overt cancerous mass, suggesting that transformed cells of the FTE may in some instances acquire a migratory and invasive phenotype before they metastasize to the ovary and begin to proliferate at an increased rate.

ChIP-sequencing revealed that BORIS preferentially bound at gene promoters and CGI, with this tendency strongest for BORIS-only sites. In addition, BORIS binding was more likely to be found at BORIS-induced DEGs, implicating BORIS in a direct regulatory role of these loci. Although ChIP-seq analyses of FT282 cells or its derivatives for histone modifications and other transcription factors have yet to be carried out, it is likely that BORIS binding sites co-localize with active chromatin marks such as H3Kme2, H3Kme3, H3K27ac, H3K79me2 and H3K9ac, in addition to the histone variant H2A.Z, as observed in other cell systems [15, 16].

Interestingly, we identified more than 500 CTCF binding sites in FT282-BORIS cells that were either undetectable in FT282-EV cells or exhibited enhanced binding in BORIS expressing cells. Roughly half of these sites were also bound by BORIS suggesting that, at least for these sites, binding of BORIS may provoke a more open chromatin conformation that facilitates CTCF binding. For the remaining new or enhanced CTCF sites that do not exhibit binding of BORIS it is possible that a similar mechanism is in play but occurred very early after the in0duction of BORIS expression where BORIS functioned in a “hit and run” fashion. The mechanism by which BORIS facilitates new or increased binding of CTCF is unknown. Consistent with evidence that BORIS binding is less sensitive to methylation [48], it is possible that BORIS promotes DNA demethyation at these regions, thereby allowing CTCF binding, as previously shown for other loci [12, 27] perhaps by recruitment of TET proteins and conversion of 5mC to 5hmC [49]. An alternative mechanisms may be that BORIS acts as a pioneer factor at these sites, either allowing CTCF to bind via protein-protein interactions, or recruiting chromatin remodelers that reposition nucleosomes to allow CTCF binding[50].

In summary, our results provide evidence supporting a pro-tumorigenic role for BORIS in HGSC. In FT282 cells, ectopic BORIS expression significantly increased cellular migration and invasion, deregulated the cell cycle, and significantly altered gene expression. We provide further support for BORIS as an important mediator of inflammation as has suggested previously and confirm that BORIS binding is not uniform across CTCF sites. Relevant future investigations of BORIS related oncogenic mechanisms should include the process by which CTCF binding is altered and the function of aberrant O-linked glycosylation of mucins.

Supplementary Material

Refer to Web version on PubMed Central for supplementary material.

Acknowledgments

We thank Ronny Drapkin (Dana-Farber Cancer Institute) for the original FT282 cell line and Tan Tuan Zea (Cancer Science Institute of Singapore) for doing custom analyses of the CSIOVBD. Funding was provided by: DOD Ovarian Cancer Research Program (W81XWH-12-1-0456), A. Karpf and M. Higgins; Teal Predoctoral Scholarship (DOD), J. Hillman; R01 Diversity supplement (3R01CA197996-02S1), S. Rosario; the Roswell Park Alliance Foundation, M. Higgins. NIH T32CA009476, C. Barger; NIH/NCI F99CA212470, C. Barger; UNMC Program of Excellence Assistantship. C. Barger. This work was also supported by Roswell Park Comprehensive Center and National Cancer Institute (NCI) grant P30CA016056 and Fred & Pamela Buffett Cancer Center NCI support grant P30CA036727. We dedicate this work to Colleen Timmins.

References

1. Patch AM, Christie EL, Etemadmoghadam D, Garsed DW, George J, Fereday S, Nones K, Cowin P, Alsop K, Bailey PJ et al.: Whole-genome characterization of chemoresistant ovarian cancer. Nature 2015, 521(7553):489–494. [PubMed: 26017449]
2. Barger CJ, Zhang W, Hillman J, Stablewski AB, Higgins MJ, Vanderhyden BC, Odunsi K, Karpf AR: Genetic determinants of FOXM1 overexpression in epithelial ovarian cancer and functional contribution to cell cycle progression. Oncotarget 2015, 6(29):27613–27627. [PubMed: 26243836]
3. Nik NN, Vang R, Shih Ie M, Kurman RJ: Origin and pathogenesis of pelvic (ovarian, tubal, and primary peritoneal) serous carcinoma. Annu Rev Pathol 2014, 9:27–45. [PubMed: 23937438]
4. Kauff ND, Barakat RR: Risk-reducing salpingo-oophorectomy in patients with germline mutations in BRCA1 or BRCA2. J Clin Oncol 2007, 25(20):2921–2927. [PubMed: 17617523]
5. Klinkebiel D, Zhang W, Akers SN, Odunsi K, Karpf AR: DNA Methylome Analyses Implicate Fallopian Tube Epithelia as the Origin for High-Grade Serous Ovarian Cancer. Mol Cancer Res 2016, 14(9):787–794. [PubMed: 27259716]
6. Karst AM, Drapkin R: Primary culture and immortalization of human fallopian tube secretory epithelial cells. Nat Protoc 2012, 7(9):1755–1764. [PubMed: 22936217]
7. Karst AM, Jones PM, Vena N, Ligon AH, Liu JF, Hirsch MS, Etemadmoghadam D, Bowtell DD, Drapkin R: Cyclin E1 deregulation occurs early in secretory cell transformation to promote formation of fallopian tube-derived high-grade serous ovarian cancers. Cancer Res 2014, 74(4): 1141–1152. [PubMed: 24366882]
8. Woloszynska-Read A, James SR, Link PA, Yu J, Odunsi K, Karpf AR: DNA methylation-dependent regulation of BORIS/CTCFL expression in ovarian cancer. Cancer Immun 2007, 7:21. [PubMed: 18095639]
9. Woloszynska-Read A, Zhang W, Yu J, Link PA, Mhawech-Fauceglia P, Collamat G, Akers SN, Ostler KR, Godley LA, Odunsi K et al.: Coordinated cancer germline antigen promoter and global DNA hypomethylation in ovarian cancer: association with the BORIS/CTCF expression ratio and advanced stage. Clin Cancer Res 2011, 17(8):2170–2180. [PubMed: 21296871]
10. Marshall AD, Bailey CG, Rasko JE: CTCF and BORIS in genome regulation and cancer. Curr Opin Genet Dev 2014, 24:8–15. [PubMed: 24657531]
11. Wang C, Gu Y, Zhang K, Xie K, Zhu M, Dai N, Jiang Y, Guo X, Liu M, Dai J et al.: Systematic identification of genes with a cancer-testis expression pattern in 19 cancer types. Nat Commun 2016, 7:10499. [PubMed: 26813108]
12. Vatolin S, Abdullaev Z, Pack SD, Flanagan PT, Custer M, Loukinov DI, Pugacheva E, Hong JA, Morse H 3rd, Schrump DS et al.: Conditional expression of the CTCF-paralogous transcriptional factor BORIS in normal cells results in demethylation and derepression of MAGE-A1 and reactivation of other cancer-testis genes. Cancer Res 2005, 65(17):7751–7762. [PubMed: 16140943]
13. Loukinov D: Targeting CTCFL/BORIS for the immunotherapy of cancer. Cancer Immunol Immunother 2018, 67(12):1955–1965. [PubMed: 30390146]

14. Loukinov DI, Pugacheva E, Vatolin S, Pack SD, Moon H, Chernukhin I, Mannan P, Larsson E, Kanduri C, Vostrov AA et al.: BORIS, a novel male germ-line-specific protein associated with epigenetic reprogramming events, shares the same 11-zinc-finger domain with CTCF, the insulator protein involved in reading imprinting marks in the soma. Proc Natl Acad Sci U S A 2002, 99(10): 6806–6811. [PubMed: 12011441]
15. Pugacheva EM, Rivero-Hinojosa S, Espinoza CA, Mendez-Catala CF, Kang S, Suzuki T, Kosaka-Suzuki N, Robinson S, Nagarajan V, Ye Z et al.: Comparative analyses of CTCF and BORIS occupancies uncover two distinct classes of CTCF binding genomic regions. Genome Biol 2015, 16(1):161. [PubMed: 26268681]
16. Bergmaier P, Weth O, Dienstbach S, Boettger T, Galjart N, Mernberger M, Bartkuhn M, Renkawitz R: Choice of binding sites for CTCFL compared to CTCF is driven by chromatin and by sequence preference. Nucleic Acids Res 2018, 46(14):7097–7107. [PubMed: 29860503]
17. Moore JM, Rabaia NA, Smith LE, Fagerlie S, Gurley K, Loukinov D, Disteche CM, Collins SJ, Kemp CJ, Lobanenkov VV et al.: Loss of maternal CTCF is associated with peri-implantation lethality of Ctcf null embryos. PLoS ONE 2012, 7(4):e34915. [PubMed: 22532833]
18. Arzate-Mejia RG, Recillas-Targa F, Corces VG: Developing in 3D: the role of CTCF in cell differentiation. Development 2018, 145(6).
19. Parelho V, Hadjur S, Spivakov M, Leleu M, Sauer S, Gregson HC, Jarmuz A, Canzonetta C, Webster Z, Nesterova T et al.: Cohesins functionally associate with CTCF on mammalian chromosome arms. Cell 2008, 132(3):422–433. [PubMed: 18237772]
20. Suzuki T, Kosaka-Suzuki N, Pack S, Shin DM, Yoon J, Abdullaev Z, Pugacheva E, Morse HC 3rd, Loukinov D, Lobanenkov V: Expression of a testis-specific form of Gal3st1 (CST), a gene essential for spermatogenesis, is regulated by the CTCF paralogous gene BORIS. Mol Cell Biol 2010, 30(10):2473–2484. [PubMed: 20231363]
21. Sleutels F, Soochit W, Bartkuhn M, Heath H, Dienstbach S, Bergmaier P, Franke V, Rosa-Garrido M, van de Nobelen S, Caesar L et al.: The male germ cell gene regulator CTCFL is functionally different from CTCF and binds CTCF-like consensus sites in a nucleosome composition-dependent manner. Epigenetics & chromatin 2012, 5(1):8. [PubMed: 22709888]
22. Rivero-Hinojosa S, Kang S, Lobanenkov VV, Zentner GE: Testis-specific transcriptional regulators selectively occupy BORIS-bound CTCF target regions in mouse male germ cells. Sci Rep 2017, 7:41279. [PubMed: 28145452]
23. Martin-Kleiner I: BORIS in human cancers -- a review. Eur J Cancer 2012, 48(6):929–935. [PubMed: 22019212]
24. Hoivik EA, Kusonmano K, Halle MK, Berg A, Wik E, Werner HM, Petersen K, Oyan AM, Kalland KH, Krakstad C et al.: Hypomethylation of the CTCFL/BORIS promoter and aberrant expression during endometrial cancer progression suggests a role as an Epi-driver gene. Oncotarget 2014, 5(4):1052–1061. [PubMed: 24658009]
25. Alberti L, Losi L, Leyvraz S, Benhattar J: Different Effects of BORIS/CTCFL on Stemness Gene Expression, Sphere Formation and Cell Survival in Epithelial Cancer Stem Cells. PLoS One 2015, 10(7):e0132977. [PubMed: 26185996]
26. Liu Q, Chen K, Liu Z, Huang Y, Zhao R, Wei L, Yu X, He J, Liu J, Qi J et al.: BORIS up-regulates OCT4 via histone methylation to promote cancer stem cell-like properties in human liver cancer cells. Cancer Lett 2017, 403:165–174. [PubMed: 28645561]
27. Gaykalova D, Vatapalli R, Glazer CA, Bhan S, Shao C, Sidransky D, Ha PK, Califano JA: Dose-dependent activation of putative oncogene SBSN by BORIS. PLoS One 2012, 7(7):e40389. [PubMed: 22792300]
28. Alberti L, Renaud S, Losi L, Leyvraz S, Benhattar J: High expression of hTERT and stemness genes in BORIS/CTCFL positive cells isolated from embryonic cancer cells. PLoS One 2014, 9(10):e109921. [PubMed: 25279549]
29. Okabayashi K, Fujita T, Miyazaki J, Okada T, Iwata T, Hirao N, Noji S, Tsukamoto N, Goshima N, Hasegawa H et al.: Cancer-testis antigen BORIS is a novel prognostic marker for patients with esophageal cancer. Cancer Sci 2012, 103(9):1617–1624. [PubMed: 22676270]
30. Lobanenkov VV, Zentner GE: Discovering a binary CTCF code with a little help from BORIS. Nucleus 2018, 9(1):33–41. [PubMed: 29077515]

31. Barger CJ, Zhang W, Sharma A, Chee L, James SR, Kufel CN, Miller A, Meza J, Drapkin R, Odunsi K et al.: Expression of the POTE gene family in human ovarian cancer. Sci Rep 2018, 8(1): 17136. [PubMed: 30459449]
32. Skehan P, Storeng R, Scudiero D, Monks A, McMahon J, Vistica D, Warren JT, Bokesch H, Kenney S, Boyd MR: New colorimetric cytotoxicity assay for anticancer-drug screening. J Natl Cancer Inst 1990, 82(13):1107–1112. [PubMed: 2359136]
33. Tan TZ, Yang H, Ye J, Low J, Choolani M, Tan DS, Thiery JP, Huang RY: CSIOVDB: a microarray gene expression database of epithelial ovarian cancer subtype. Oncotarget 2015, 6(41):43843–43852. [PubMed: 26549805]
34. Lee Y, Miron A, Drapkin R, Nucci MR, Medeiros F, Saleemuddin A, Garber J, Birch C, Mou H, Gordon RW et al.: A candidate precursor to serous carcinoma that originates in the distal fallopian tube. J Pathol 2007, 211(1):26–35. [PubMed: 17117391]
35. Currie E, Schulze A, Zechner R, Walther TC, Farese RV Jr.: Cellular fatty acid metabolism and cancer. Cell Metab 2013, 18(2):153–161. [PubMed: 23791484]
36. Li T, Guo H, Song Y, Zhao X, Shi Y, Lu Y, Hu S, Nie Y, Fan D, Wu K: Loss of vinculin and membrane-bound beta-catenin promotes metastasis and predicts poor prognosis in colorectal cancer. Mol Cancer 2014, 13:263. [PubMed: 25496021]
37. Hakomori S: Glycosylation defining cancer malignancy: new wine in an old bottle. Proc Natl Acad Sci U S A 2002, 99(16):10231–10233. [PubMed: 12149519]
38. Wang R, Yu C, Zhao D, Wu M, Yang Z: The mucin-type glycosylating enzyme polypeptide N-acetylgalactosaminyltransferase 14 promotes the migration of ovarian cancer by modifying mucin 13. Oncol Rep 2013, 30(2):667–676. [PubMed: 23708057]
39. Qi CF, Martensson A, Mattioli M, Dalla-Favera R, Lobanenkov VV, Morse HC 3rd: CTCF functions as a critical regulator of cell-cycle arrest and death after ligation of the B cell receptor on immature B cells. Proc Natl Acad Sci U S A 2003, 100(2):633–638. [PubMed: 12524457]
40. Heath H, Ribeiro de Almeida C, Sleutels F, Dingjan G, van de Nobelen S, Jonkers I, Ling KW, Gribnau J, Renkawitz R, Grosveld F et al.: CTCF regulates cell cycle progression of alphabeta T cells in the thymus. EMBO J 2008, 27(21):2839–2850. [PubMed: 18923423]
41. Roy AR, Ahmed A, DiStefano PV, Chi L, Khyzha N, Galjart N, Wilson MD, Fish JE, Delgado-Olguin P: The transcriptional regulator CCCTC-binding factor limits oxidative stress in endothelial cells. J Biol Chem 2018, 293(22):8449–8461. [PubMed: 29610276]
42. Blackford AN, Jackson SP: ATM, ATR, and DNA-PK: The Trinity at the Heart of the DNA Damage Response. Mol Cell 2017, 66(6):801–817. [PubMed: 28622525]
43. Huanna T, Tao Z, Xiangfei W, Longfei A, Yuanyuan X, Jianhua W, Cuifang Z, Manjing J, Wenjing C, Shaochuan Q et al.: GALNT14 mediates tumor invasion and migration in breast cancer cell MCF-7. Mol Carcinog 2015, 54(10):1159–1171. [PubMed: 24962947]
44. Woloszynska-Read A, Mhawech-Fauceglia P, Yu J, Odunsi K, Karpf AR: Intertumor and intratumor NY-ESO-1 expression heterogeneity is associated with promoter-specific and global DNA methylation status in ovarian cancer. Clin Cancer Res 2008, 14(11):3283–3290. [PubMed: 18519754]
45. Hong JA, Kang Y, Abdullaev Z, Flanagan PT, Pack SD, Fischette MR, Adnani MT, Loukinov DI, Vatolin S, Risinger JI et al.: Reciprocal Binding of CTCF and BORIS to the NY-ESO-1 Promoter Coincides with Derepression of this Cancer-Testis Gene in Lung Cancer Cells. Cancer Res 2005, 65(17):7763–7774. [PubMed: 16140944]
46. Woloszynska-Read A, James SR, Song C, Jin B, Odunsi K, Karpf AR: BORIS/CTCFL expression is insufficient for cancer-germline antigen gene expression and DNA hypomethylation in ovarian cell lines. Cancer Immun 2010, 10:6. [PubMed: 20649179]
47. Kholmanskikh O, Loriot A, Brasseur F, De Plaen E, De Smet C: Expression of BORIS in melanoma: lack of association with MAGE-A1 activation. Int J Cancer 2008, 122(4):777–784. [PubMed: 17957795]
48. Nguyen P, Cui H, Bisht KS, Sun L, Patel K, Lee RS, Kugoh H, Oshimura M, Feinberg AP, Gius D: CTCFL/BORIS is a methylation-independent DNA-binding protein that preferentially binds to the paternal H19 differentially methylated region. Cancer Res 2008, 68(14):5546–5551. [PubMed: 18632606]

49. Teif VB, Beshnova DA, Vainshtein Y, Marth C, Mallm JP, Hofer T, Rippe K: Nucleosome repositioning links DNA (de)methylation and differential CTCF binding during stem cell development. Genome Res 2014, 24(8):1285–1295. [PubMed: 24812327]

50. Wiechens N, Singh V, Gkikopoulos T, Schofield P, Rocha S, Owen-Hughes T: The Chromatin Remodelling Enzymes SNF2H and SNF2L Position Nucleosomes adjacent to CTCF and Other Transcription Factors. PLoS Genet 2016, 12(3):e1005940. [PubMed: 27019336]

Implications

These studies provide evidence that aberrant expression of BORIS may play a role in the progression to HGSC by enhancing the migratory and invasive properties of FTSEC.

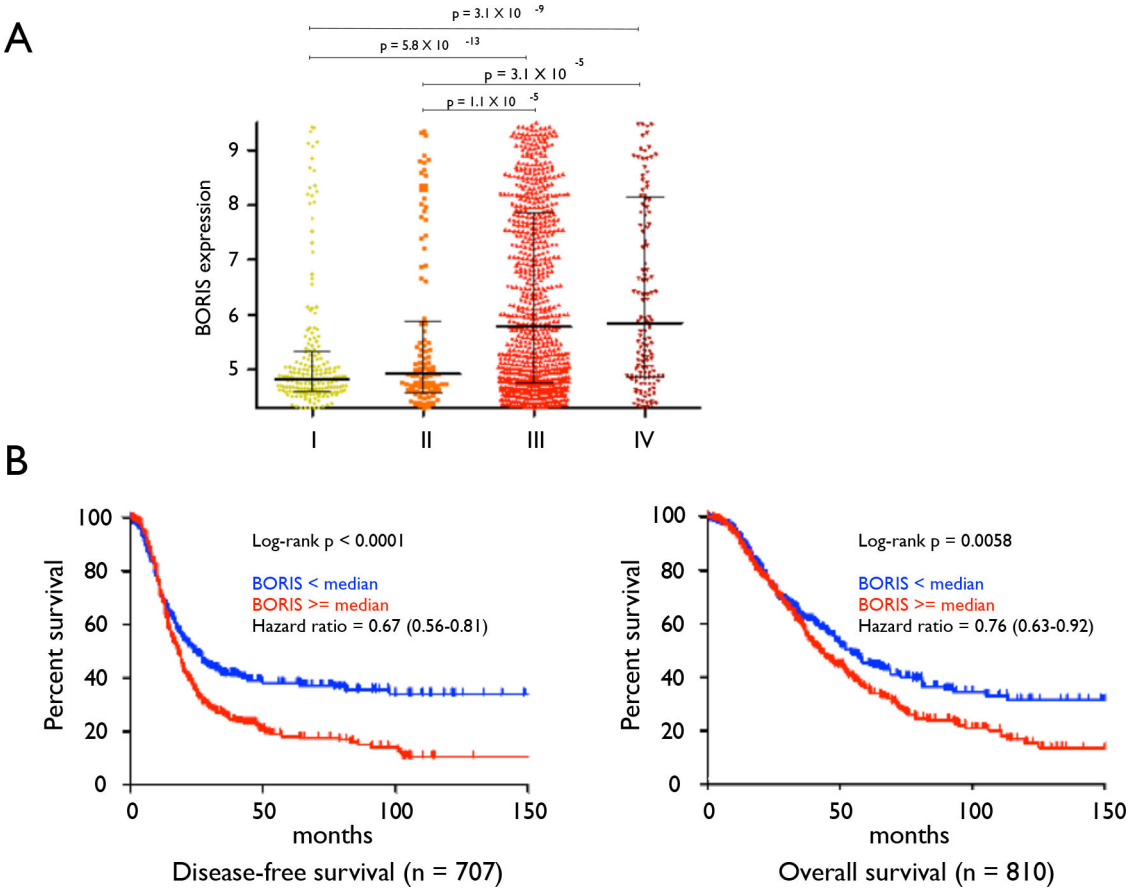

Figure 1. *BORIS* expression correlates with increased tumor stage and reduced survival in CSIOVDB.

(A) Analysis of tumor stage. *BORIS* expression is significantly higher in stage III and IV tumors compared to stage I and II tumors. Units on the vertical axis represent normalized intensity. Statistical analysis by Mann Whitney test. (B) Kaplan-Meier analysis of patient samples partitioned into two groups based on the median expression of *BORIS*. Left-hand curves show disease-free survival (n = 708); right-hand curves show overall survival (n =810).

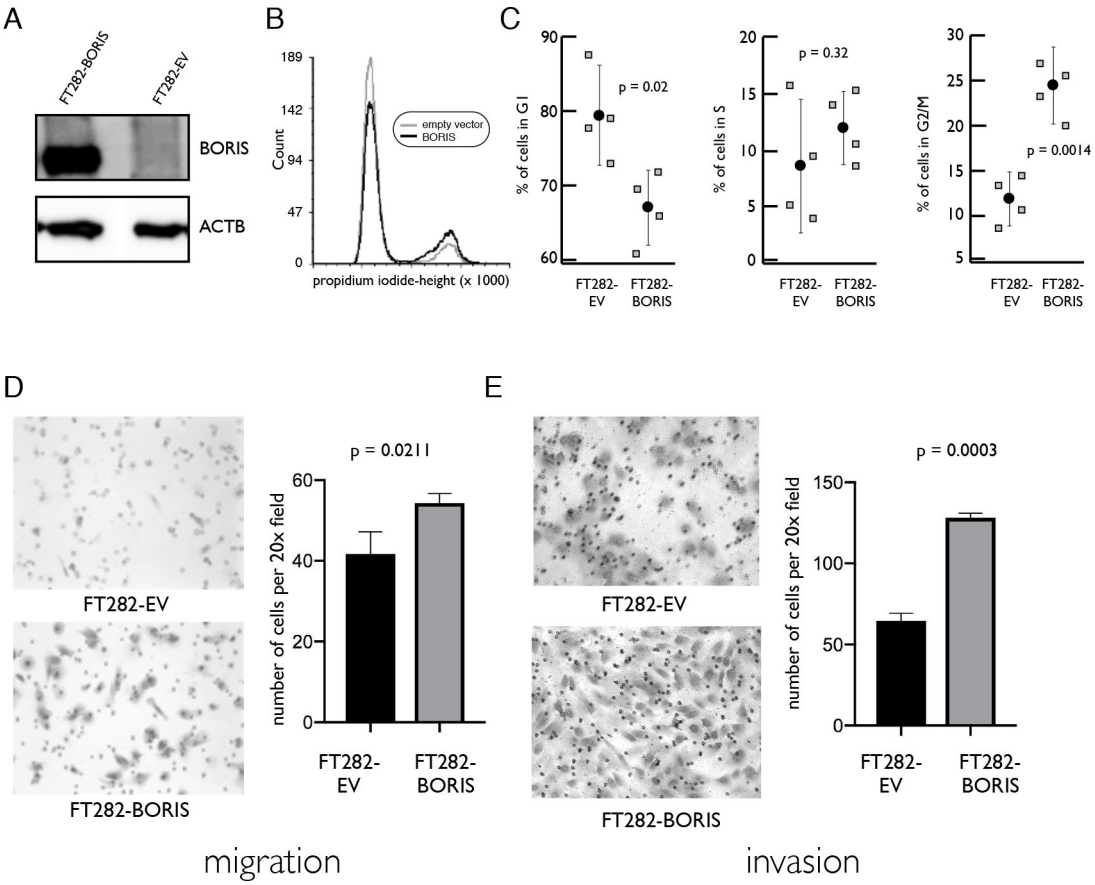

Figure 2. Ectopic expression of *BORIS* in FT282 cells results in cell cycle arrest, increased cellular motility, and greater invasion capability.

FT282 cells were transduced with a lentivirus containing a CpG-free BORIS cDNA, or with the empty vector, grown for 14 days and enriched for GFP expressing cells by FACS. (A) Western blot analysis using antibodies to BORIS or β-actin (ACTB). (B) Approximately $2X10^6$ FT282-EV or FT282-BORIS cells were fixed in ethanol, stained with propidium iodide and analyzed on a LSR Fortessa instrument; representative FACS profile of DNA content (propidium iodide staining) of FT282-EV and FT282-BORIS cells. (C)The average proportion of cells in G1, S, or G2/M for 4 replicates and the individual values for each replicate are shown. Statistical analysis was done using an unpaired student's t test. (D) Approximately 5 X 10^4 cells in 500 μl serum-free medium were pipetted into the top of transwell inserts in a 24 well plate with the lower chamber contained 500 μl complete medium. After incubation for 18hr, the membranes were washed, fixed and stained with crystal violet. Representative microphotographs of the bottom surface of the membranes are shown (left). The average number of cells on the bottom surface of the membrane was determined by microscopic examination of 3 biological replicates (four 20x fields each, right panel). Statistical analysis was done using an unpaired student's t test. (E) Invasion assays were done in a manner similar to the transwell motility assays but using inserts coated with Matrigel. The number of cells per 20x field represents the mean and SD of 3 biological replicates (four 20x fields per replicate). Statistical analysis was done using an unpaired student's t test.

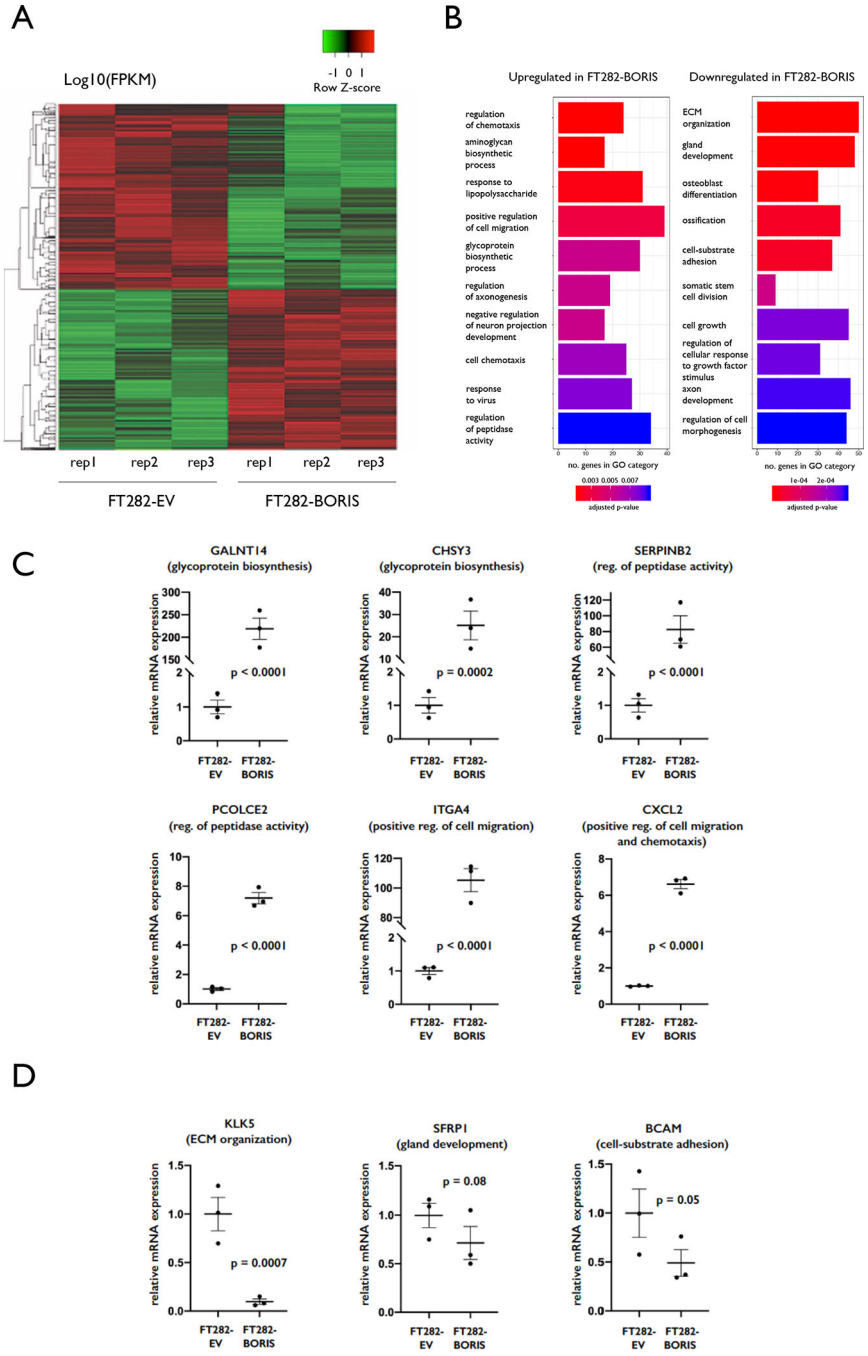

Figure 3. Ectopic expression of BORIS in FT282 cells induces gene expression changes in biological processes associated with cancer

(A) RNA-seq was carried out on FT282-EV and FT282-BORIS cells using 3 independent RNA isolates each. Differentially expressed genes between FT282-EV and FT282-BORIS cells (q-value < 0.05 and the log2 fold change > ± 0.25) were used to generate the heat map. (B) Bar plots of GO analysis. The length of the bar indicates the number of DEGs in each enriched category and the color of each bar indicates the adjusted p-value for each ontology. (C&D) RT-qPCR results for 6 genes corresponding to upregulated GO categories (C) and 3 genes for downregulated categories (D). For each gene there were 3 “biological” replicates

(i.e. 3 cell cultures, 3 RNA preps, 3 cDNA syntheses) and 3 technical replicates biological replicate. The plots show the mean expression level in FT282-BORIS cells relative to FT282-EV cells and SE of the 3 biological replicates; the solid dots are the individual replicates. Statistical analysis was by unpaired t-test.

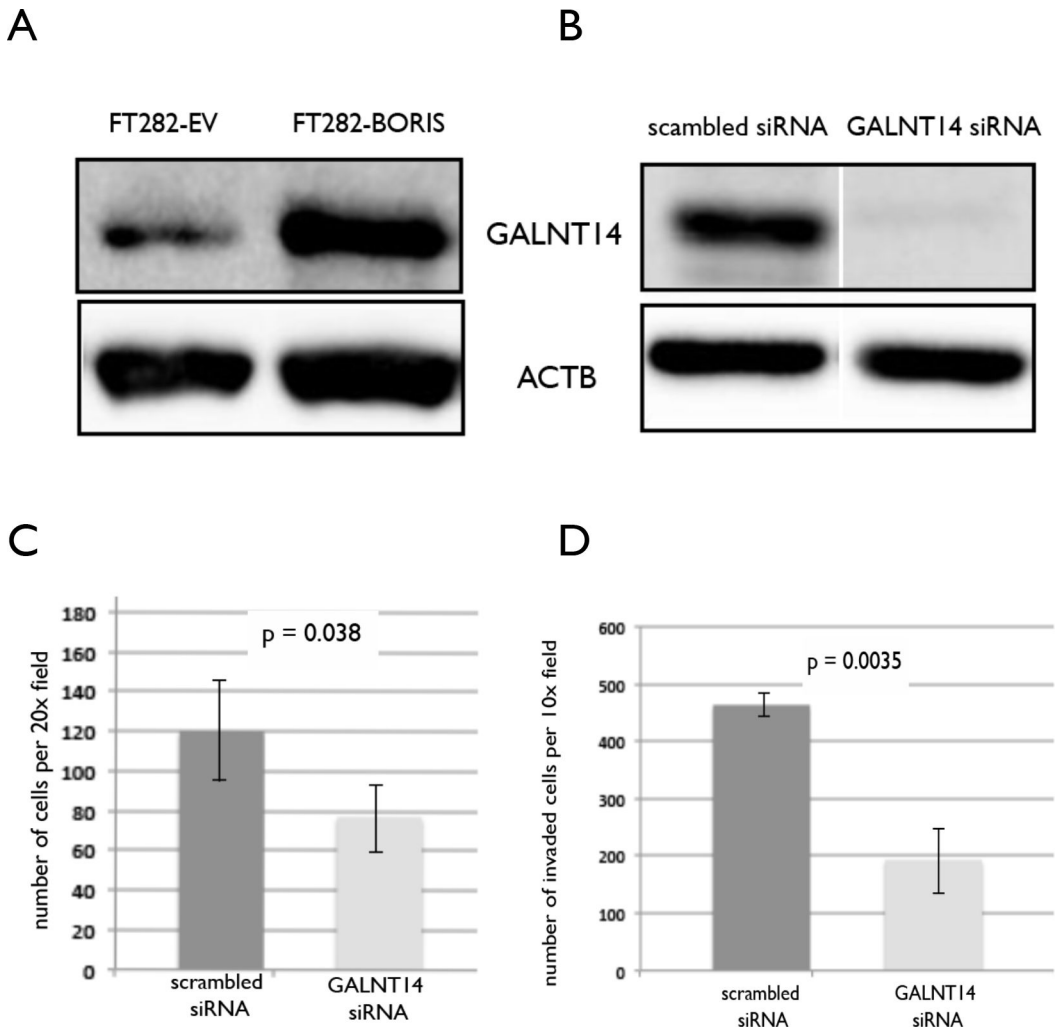

Figure 4. Increased motility and invasion induced by ectopic expression of BORIS is partially attributable to increased expression of GALNT14.

(A) Western blot analysis of FT282-EV and FT282-BORIS cells using antibodies for GALNT14 and β-actin. (B) Western blot of FT282-BORIS cells 48 hr after transfection with Silencer® Select Negative Control 1 (scrambled) siRNA or Silencer® Select siRNA targeted against GALNT14. (C) Transwell migration assays were carried out as described in the legend to Figure1 using FT282-BORIS cells treated with scrambled siRNA control or GALNT14 siRNA. The average number of cells on the bottom surface of the membrane was determined by microscopic examination of 3 biological replicates (four 20x fields each). Statistical analysis was done using an unpaired student's t test. (D) Invasion assays were carried out as described in the legend to Figure1 using FT282-BORIS cells treated with scrambled siRNA control or GALNT14 siRNA. The number of cells per 20x field represents the mean and SD of 3 biological replicates (four 20x fields per replicate). Statistical analysis was done using a t test.

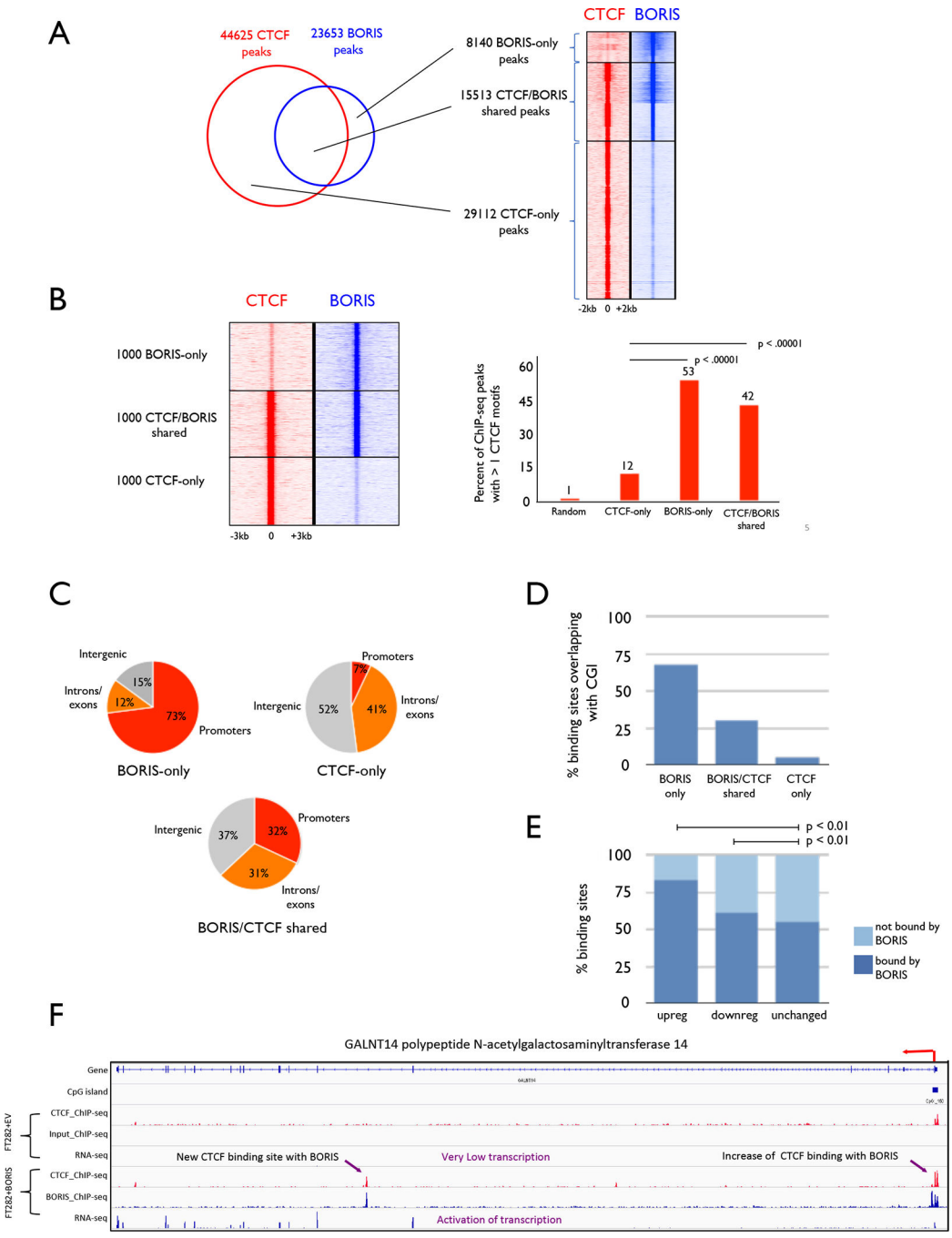

Figure 5. Ectopically expressed BORIS binds to a subset of CTCF sites enriched in > 1 CTCF binding motif.

(A) Left, Venn diagram depicting overlap of CTCF and BORIS binding sites in FT282-BORIS cells determined by ChIP-seq. **Right,** Heatmap depicts CTCF (red) and BORIS (blue) occupancy at 55061 loci in FT282-BORIS cells. The tag density of CTCF and BORIS ChIP-seq data was collected within a 4-kb window around the summit of CTCF (CTCF&BORIS and CTCF-only) and BORIS peaks (BORIS-only). The collected data were subjected to k-means clustering using linear normalization based on similar tag density

profiles using seqMiner. **(B) Left,** Heat map showing ChIP-seq tag density at the top 1000 CTCF-only, BORIS-only, and CTCF/BORIS peaks chosen for CTCF motif analysis. **Right,** Proportion of peaks in each class found by FIMO (MEME suite) to contain > 1 CTCF motif. Statistical analysis by Chi-squared test. **(C)** Genomic distribution of the three classes of CTCF and BORIS binding sites in FT282 cells ectopically expressing BORIS. **(D)** Prevalence of CTCF and BORIS binding sites at CpG islands in FT282-BORIS cells. **(E)**. Proportions of differentially expressed genes bound by BORIS FT282-BORIS cells. Comparisons tested for significance by Chi Square analysis. **(F)** The *GALNT14* locus shows enhancement of CTCF binding at its promoter and the appearance of a “new” CTCF binding site associated with enhanced gene expression following binding of BORIS.